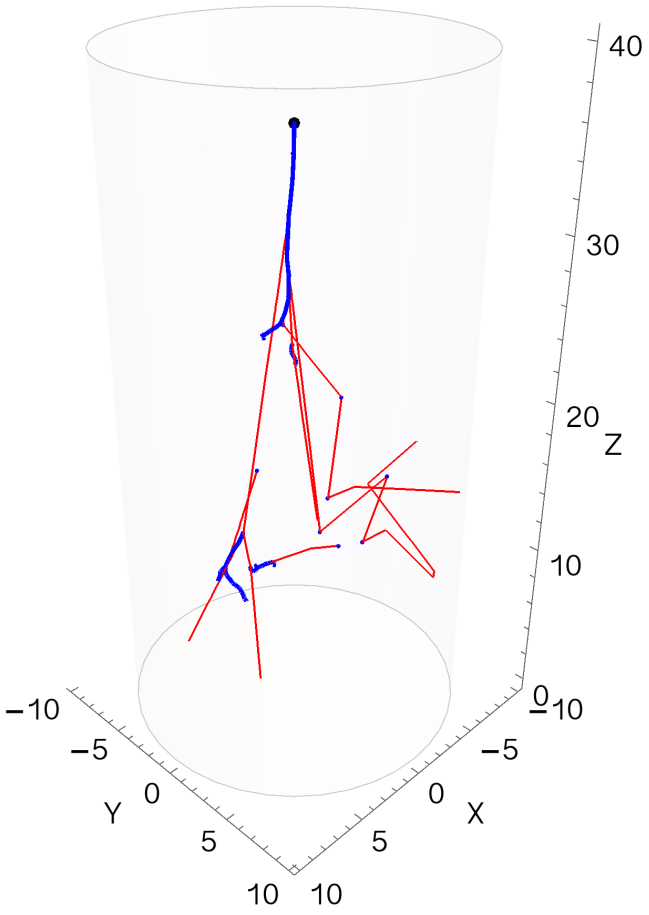

MaPLE

A **Ma**thematica simulation of **P**hoton and **L**epton **E**nergy-deposition

Neal Woo[⋆] *and John Essick*

[⋆]electronic address: neal.d.woo@gmail.com

Contents

Introduction

This manual was written to supplement **MaPLE**, a Monte Carlo simulation of muon decay in large-volume scintillation detectors. The simulation is intended for use by advanced undergraduate students (and their institutions) to conduct experiments in measuring the muon's mass. **MaPLE** was written in Mathematica for transparency and ease-of-use, bypassing the steep learning curve and other difficulties associated with high-level particle physics codes.

The muon mass experiment is a logical extension to the already popular muon lifetime experiment[2], adding great depth and introducing some more sophisticated topics in particle physics and research methods. In this manual we present the theories, equations, and algorithms used by the simulation.

MaPLE is a mixed-class simulation of photon and electron transport in plastic scintillation detectors. Photons are simulated as undergoing three interactions: Compton scattering, photoelectric absorption, and electron-positron pair production. Electrons and positrons undergo inelastic scattering, bremsstrahlung emission, two-photon positron-electron annihilation, and multiple elastic scattering, which is treated on the basis of the alternating random-hinge method used in PENELOPE.[7] Inelastic scattering and bremsstrahlung emission with energy losses below specified thresholds are treated as continuous rather than discrete events, resulting in energy deposition to the scintillator.

The simulation is intended to be used with cylindrical, PVT-based scintillation detectors. The cylinder should ideally be large enough to capture even the most energetic secondary electrons; our experiment used a detector with radius $R_d = 10$ cm and height $H_d = 40$ cm, but this is not a requirement. If a non-cylindrical detector geometry is used, the code will need to be modified in certain places, which should be fairly straightforward. This program will not work for non-PVT based scintillators.

The rest of this introduction reviews some fundamental tools for particle physics. To skip directly to the Monte Carlo simulation, see Section 4.3.

Interactions, Cross Sections, and Sampling

For any given particle interaction, the *differential cross section* $d\sigma/dn$ expresses the intrinsic 'strength' of the interaction. The quantity $d\sigma/dn$ is a function of the variable n (which, for example, might be the outgoing solid angle) and when this differential cross section is integrated over a chosen range of n, the

total cross section σ of the interaction is determined. The total cross section has dimensions of L^2, hence the term 'area', although this association is purely hypothetical. The total cross section represents the *strength* or *likelihood* of the interaction to occur in that chosen range of n.

Suppose that a particle A traverses an infinite medium composed of particles of type B with number density N_B, and that particles A and B interact through some fictitious force f with differential cross section $d\sigma_f/d\Omega$. By convention, $d\Omega$ represents the differential solid angle into which A is scattered, $d\Omega = \sin\theta\, d\theta\, d\phi$.

Let's further suppose that we want to know how far A travels through the material before interacting, to any degree, with one of the B particles. By integrating $d\sigma_f$ over all of $d\Omega$ (that is, over $0 < \theta < \pi$ and $0 < \phi < 2\pi$), and then multiplying by the number density of target (B) particles, we get the *macroscopic cross section* Σ_f:

$$\Sigma_f = N_B\, \sigma_f = N_B \int \frac{d\sigma_f}{d\Omega}\, d\Omega\ , \tag{1}$$

with dimensions of L^{-1}. From this, we can calculate the mean free path λ_f, which is the average length between successive interactions experienced by the particle A:

$$\lambda_f = \Sigma_f^{-1} = \frac{1}{N_B\, \sigma_f}\ . \tag{2}$$

The actual length that A travels between successive interactions is determined probabilistically, according to an exponential distribution; the probability for A to travel a distance x and *not* interact decreases as e^{-x/λ_f}. For the simulation to be physically accurate, it must pick path lengths s in a way that reflects this probability. The quickest way to choose s randomly is to generate a random number $\xi \in [0, 1]$ and set

$$s = \frac{-\ln \xi}{\Sigma_f}\ . \tag{3}$$

This process is one example of what is generally called *sampling a distribution*. In this case, we sampled a path length s from the probability distribution describing the likelihood of interaction between A and B. If A and B interacted through multiple forces, we could take this same approach, but instead use the *total* macroscopic cross Σ_t for all of the interactions:

$$\Sigma_t = \Sigma_{1+2+3+\ldots} \equiv \Sigma_1 + \Sigma_2 + \Sigma_3 + \ldots \tag{4}$$

After A travels distance s in its initial direction, we have to sample the *event*, i.e., choose which interaction occurs in a manner that is both random and proportional to the relative sizes of their macroscopic cross sections.

The approach used in **MaPLE** is to generate a random number ξ from 0 to Σ_t. If ξ falls between 0 and Σ_1, then the particle suffers an interaction of type 1. If $\Sigma_1 < \xi < \Sigma_{1+2}$, it suffers an interaction of type 2. If $\Sigma_{1+2} < \xi < \Sigma_{1+2+3}$, it suffers an interaction of type 3, and so on.

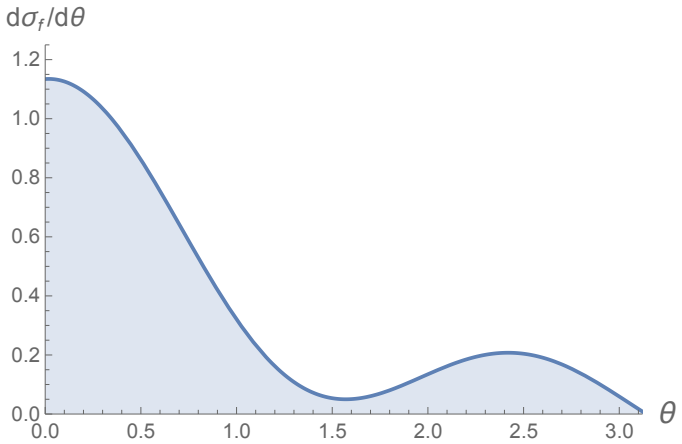

Figure 1: Plot of the differential cross section for a fictitious interaction $d\sigma_f/dn$, where dn is the differential polar scattering angle $d\theta$ (in radians).

Once s and the interaction type are known, the last step is to sample the *interaction* itself, which means determining the kinematics of the interaction, based on the profile of the differential cross section.[1] In Figure 1, we've plotted a made-up differential cross section for our fictitious force f. Here, the differential cross section is a function of θ, the polar angle into which A is scattered by the interaction.

Figure 1 is helpful for visualizing the role of the differential cross section. From this plot, we see that the particle is most likely to be scattered by a small polar angle, from $\theta = 0$ to $\theta \approx 0.75$ rad. We also see that there is some likelihood that A will 'back-scatter', most often by an angle $\theta \approx 2.4$ rad, and that it is very unlikely for A to be deflected perpendicularly at $\theta \approx 1.6$ rad.

There is no one procedure for sampling the differential cross section, because each interaction is different, and differential cross sections generally change shape based on the energy scale of the interaction. One simple sampling method is called *rejection sampling*. A point (x, y) is chosen at random, with x in the domain of $d\theta$ (x between 0 and π), and y between 0 and Max$[d\sigma_f]$. If the point (x, y) falls in the shaded region below the curve, then accept $x = \theta$. If (x, y) is above the cross section curve, reject the point and randomly pick another one. This procedure only works with some efficiency, based on the shape and characteristics of $d\sigma_f/d\theta$. Much of **MaPLE** borrows sophisticated algorithms from other codes, in order to sample interactions in a computationally efficient way.

[1] The differential cross section is not always differential in $d\Omega$, but instead can be a function of any variables related to the interaction, some of which may be more convenient to work with than others.

Chapter 1

Photon Interactions

The following definitions are used throughout this chapter:

$m_e c^2$	= electron rest mass energy
r_0	= classical electron radius
α	= fine structure constant
k	= incident photon energy
κ	$= k/m_e c^2$ = reduced incident photon energy
k_c	= Compton-scattered photon energy
Z	= atomic number of target atom
β	$= v/c$ = electron velocity in units of c
γ	$= 1/\sqrt{1-\beta^2}$ = Lorentz factor

Photons are simulated as undergoing three interactions: Compton scattering, photoelectric absorption, and positron-electron pair production. Compton scattering is the dominant process, while photoelectric absorption terminates photons when they reach extremely low energies. Pair production has a higher energy threshold and is infrequent.

Having no charge, photons travel through the detector material with ease, moving from interaction point to interaction point in straight lines. Thus, one need only predict the distance to the next interaction, move the photon forward, sample the interaction, and modify the particle properties accordingly.

Macrosopic cross sections for the three interactions[1] are provided in the table `photontable.csv`. The table is loaded into Mathematica under the symbolic name **`photontable`**. Each entry in the table has four elements $\{k, \Sigma_c, \Sigma_{pe}, \Sigma_{pp}\}$, where k is the photon energy at which the cross sections are calculated. The table covers values of k from 0.05 MeV up to 120 MeV in increments of 0.05 MeV. If a different energy range or partitioning is desired, you can generate your own table as detailed in Section 1.5.

[1] Σ_c, Σ_{pe}, and Σ_{pp} for the Compton, photoelectric, and pair-production interactions, respectively.

1.1 Compton Scattering

Compton scattering refers to photon-electron scattering with some energy transferred to the electron. A photon of energy k MeV scatters from a 'target' electron, leaving with energy $k' = k - T$. The electron then has total energy $E_e = m_e c^2 + T$ after the collision. Both particles are scattered by polar and azimuthal angles θ and ϕ, relative to the direction of travel of the incident photon. In the energy range of interest, the target electron, which is bound in an atom with atomic number Z, can be approximated as free and initially at rest.

1.1.1 Macroscopic Cross Section

The Compton scattering macroscopic cross section, Σ_c, is invoked by the command Σ**compton[**k**]**, which interpolates the cross section at incident energy k from **photontable**. The values of Σ_c are calculated by integrating the Klein-Nishina differential cross section, which is differential in the cosine of the photon's polar scattering angle, $u = \cos\theta$:

$$\frac{d\sigma_c}{du} = \pi r_0^2 Z \left(\frac{k_c}{k}\right)^2 \left(\frac{k_c}{k} + \frac{k}{k_c} + u^2 - 1\right) , \tag{1.1}$$

where k_c is the energy of the photon Compton-scattered to angle θ by an atom of atomic number Z,

$$k_c = \frac{k}{1 + k(1-u)} . \tag{1.2}$$

The plastic scintillator base PVT contains $N_H = 5.17 \times 10^{22}$ hydrogen atoms per cm^3 and $N_C = 4.69 \times 10^{22}$ carbon atoms per cm^3. Thus, Σ_c is constructed as

$$\Sigma_c(k) = N_H \int_{-1}^{1} \frac{d\sigma_c(Z=1,k)}{du} du + N_C \int_{-1}^{1} \frac{d\sigma_c(Z=6,k)}{du} du . \tag{1.3}$$

1.1.2 Sampling Algorithm

The procedure for sampling the Compton interaction is borrowed from the GEANT4 physics reference manual.[3] The algorithm is invoked by the command **comptonRXN[*k*]**, which simulates the Compton interaction of a photon with energy k and returns a list of the form: $\{\{0, k', \theta_\gamma, \phi_\gamma\}, \{-1, E_e, \theta_e, \phi_e\}\}$, describing the kinematics of the interaction.[2]

The procedure for sampling the energy is a rejection method based on the parameterization of energy transfer $\epsilon = k'/k$:

[2] k' and E_e are the final energies of the photon and electron, while 0 and -1 denote their charges. Each particle is scattered by its own polar and azimuthal angles relative to the initial direction of the photon. For consistency, all sampling algorithms return lists of this format describing the secondary particles.

(i) The lower bound of ϵ is calculated as

$$\epsilon_0 = \frac{m_e c^2}{m_e c^2 + 2k} \,, \tag{1.4}$$

so that $\epsilon \in [\epsilon_0, 1]$. Then, the parameters α_1, α_2 are calculated and the probability density functions $f_1(\epsilon)$, $f_2(\epsilon)$ are defined:

$$\begin{aligned} \alpha_1 &= \ln(1/\epsilon_0) & f_1(\epsilon) &= 1/(\alpha_1 \epsilon) \\ \alpha_2 &= (1 - {\epsilon_0}^2)/2 & f_2(\epsilon) &= \epsilon/\alpha_2 \end{aligned} \tag{1.5}$$

(ii) A random number $r_1 \in [0, 1]$ is generated. If $r_1 < \alpha_1/(\alpha_1 + \alpha_2)$, we sample from $f_1(\epsilon)$, else from $f_2(\epsilon)$.

(iii) A second random number $r_2 \in [0, 1]$ is generated. A value of ϵ is sampled either from $f_1(\epsilon)$ by choosing $\epsilon = {\epsilon_0}^{r_2}$, or from $f_2(\epsilon)$ by choosing $\epsilon = \sqrt{{\epsilon_0}^2 + (1 - {\epsilon_0}^2) r_2}$.

(iv) The rejection function $g(\epsilon)$ is calculated for the sampled value of ϵ:

$$g(\epsilon) = \left(1 - \frac{\epsilon}{1 + \epsilon^2}\, t\,(2 - t)\right) , \tag{1.6}$$

where $t = m_e c^2 (1 - \epsilon)/(k\,\epsilon)$.

(v) A third random number $r_3 \in [0, 1]$ is generated. If $g(\epsilon) \geq r_3$, then we accept the value of ϵ and set $k' = k\,\epsilon$. Otherwise, return to step (ii).

With k' sampled, the electron's final energy is set to $E_e = m_e c^2 + (k - k')$. The polar scattering angles are then calculated by

$$\begin{aligned} \theta_\gamma &= \arccos\left(1 + \frac{m_e c^2}{k} - \frac{m_e c^2}{k'}\right) , \\ \theta_e &= \arccos\left(\frac{k - k' \cos\theta_\gamma}{\sqrt{k^2 + k'^2 - 2k\,k' \cos\theta_\gamma}}\right) , \end{aligned} \tag{1.7}$$

and the azimuthal angles ϕ_γ and ϕ_e are picked randomly and opposite to each other due to conservation of momentum in the scattering plane.

1.2 Photoelectric Absorption

Photoelectric absorption occurs when a photon of energy k is absorbed by some target atom of atomic number Z, causing the ejection of an electron with total energy $E_e = m_e c^2 + k$ and, hence, Lorentz factor $\gamma = E_e/m_e c^2$. As with Compton scattering, binding energy is neglected. The electron is emitted in some new direction due to the underlying momentum distribution of bound electrons.

1.2.1 Total Cross Section

The macroscopic cross section for photoelectric absorption, Σ_{pe}, is invoked by the command Σ**pe[**k**]**, which interpolates from the table **photontable**. The values for Σ_{pe} are calculated by integrating the Sauter differential cross section, which is differential in the emitted electron solid angle $d\Omega_e = \sin\theta_e \, d\theta_e \, d\phi_e$:

$$\frac{d\sigma_{pe}}{d\Omega_e} = \alpha^4 r_0^2 \Big(\frac{Z}{\kappa}\Big)^5 \frac{\beta^3}{\gamma} \frac{\sin^2\theta_e}{(1-\beta\cos\theta_e)^4} \Big[1 + \frac{1}{2}\gamma(\gamma-1)(\gamma-2)(1-\beta\cos\theta_e)\Big] \, . \tag{1.8}$$

As in Eq. (1.3), the integrations are carried out over the entire angular range for both $Z = 1$ and $Z = 6$, then multiplied by N_H and N_C to construct Σ_{pe}.

1.2.2 Sampling Algorithm

The procedure for sampling the photoelectron's direction is borrowed from GEANT4.[3] The algorithm is invoked by the command **peRXN[**k**]**, which returns a list of the form: $\big\{\{-1, E_e, \theta_e, \phi_e\}\big\}$, describing the photoelectron's final energy and angular deflection. The algorithm is based on the Sauter-Gavrila distribution of K-shell electrons, which is accurate enough for our energy range.

The algorithm is a rejection method based on the parameterization of the electron's Lorentz factor, $b = \gamma(\gamma-1)(\gamma-2)/2$:

(i) The parameter b is calculated for the electron with energy $E_e = m_e c^2 + k$ and Lorentz factor $\gamma = E_e/m_e c^2$.

(ii) The cosine of the polar emission angle is sampled from a probability density function by generating a random number $r_1 \in [0,1]$ and choosing

$$\cos\theta_e = \frac{(1-2r_1)+\beta}{(1-2r_1)\beta+1} \, . \tag{1.9}$$

where $\beta = v/c$.

(iii) The rejection function $g(\cos\theta_e)$ is calculated for the sampled value by

$$g(\cos\theta_e) = \frac{1-(\cos\theta_e)^2}{(1-\beta\cos\theta_e)^2}\big(1 + b(1-\beta\cos\theta_e)\big) \, . \tag{1.10}$$

(iv) A second random number $r_2 \in [0,1]$ is generated. If $g(\cos\theta_e) \geq r_2$, we accept the value of $\cos\theta_e$. Otherwise, return to step (ii).

With θ_e sampled, we then pick ϕ_e randomly between 0 and 2π.

1.3 Pair Production

Electron-positron pair production occurs due to the absorption of a high-energy photon in the vicinity of an atomic nucleus. The process can occur either in the field of the nucleus, where the threshold photon energy for pair production is $2m_ec^2$, or by interaction with a bound atomic electron. The latter is called 'triplet production' as it produces *two* electrons and one positron, due to the recoil of the target electron; the threshold energy for triplet production is $4m_ec^2$.

1.3.1 Total Cross Section

The macroscopic cross section for pair production, Σ_{pp}, is invoked by the command Σ**pp[**k**]**, which interpolates from **photontable**. The values for Σ_{pp} are calculated by integrating a modified form of the Bethe-Heitler differential cross section, which is differential in the parameter $\epsilon = (T + m_ec^2)/k$, where T is the kinetic energy of the produced electron:

$$\frac{d\sigma_{pp}}{d\epsilon} = r_0^2\,\alpha\,Z\big[Z+\eta(Z)\big]\,C_r\,\frac{2}{3}\left[2\left(\frac{1}{2}-\epsilon\right)^2\phi_1(\epsilon)+\phi_2(\epsilon)\right], \tag{1.11}$$

where $C_r = 1.0093$ is the high-energy radiative correction[3] term.

The $\eta(Z)$ parameter represents the contribution due to triplet production, and is empirically expressed as

$$\eta(Z) = (1-e^{-v})\eta_\infty\,, \tag{1.12}$$

where $\eta_\infty = 1.157$ for $Z = 1$ and $\eta_\infty = 1.174$ for $Z = 6$. The parameter v is expressed as

$$\begin{aligned} v =&(0.284-0.1909a)\ln(4/\kappa) + (0.1095+0.2206a)\ln^2(4/\kappa) \\ &+ (0.02888-0.04269a)\ln^3(4/\kappa) + (0.002527+0.002623a)\ln^4(4/\kappa)\,, \end{aligned} \tag{1.13}$$

with $\kappa = k/m_ec^2$ and $a = \alpha Z$.

Lastly, the terms $\phi_1(\epsilon)$ and $\phi_2(\epsilon)$ are defined by

$$\begin{aligned} \phi_1(\epsilon) &= g_1(b) + g_0(\kappa)\,, \\ \phi_2(\epsilon) &= g_2(b) + g_0(\kappa)\,, \end{aligned} \tag{1.14}$$

where

$$\begin{aligned} g_1(b) =&\frac{7}{3} - 2\ln(1+b^2) - 6b\arctan(b^{-1}) \\ &- b^2\Big(4 - 4b\arctan(b^{-1}) - 3\ln(1+b^{-2})\Big)\,, \\ g_2(b) =&\frac{11}{6} - 2\ln(1+b^2) - 3b\arctan(b^{-1}) \\ &+ \frac{b^2}{2}\Big(4 - 4b\arctan(b^{-1}) - 3\ln(1+b^{-2})\Big)\,, \end{aligned} \tag{1.15}$$

[3] Atrributed to Mork and Olsen.[5]

and

$$g_0(\kappa) = 4\ln(\tilde{R}) - 4f_C(Z) + F_0(\kappa, Z)\ . \tag{1.16}$$

The parameters used in these terms are defined as:

$$b = \tilde{R}\,\frac{1}{2\kappa}\,\frac{1}{\epsilon(1-\epsilon)} \tag{1.17}$$

$$\begin{aligned} f_C(Z) =& a^2\Big[(1+a^2)^{-1} + 0.202059 - 0.03693a^2 + 0.00835a^4 \\ & - 0.00201a^6 + 0.00049a^8 - 0.00012a^{10} + 0.00003a^{12}\Big] \end{aligned} \tag{1.18}$$

$$\begin{aligned} F_0(\kappa, Z) =& (-0.1774 - 12.10a + 11.18a^2)(2/\kappa)^{1/2} \\ & + (8.523 + 73.26a - 44.41a^2)(2/\kappa) \\ & - (13.52 + 121.1a - 96.41a^2)(2/\kappa)^{3/2} \\ & + (8.946 + 62.05a - 63.41a^2)(2/\kappa)^2 \end{aligned} \tag{1.19}$$

with the reduced screening radius[4] $\tilde{R}$ taking values $\tilde{R} = 122.81$ for $Z = 1$ and $\tilde{R} = 61.228$ for $Z = 6$. Values for the Z-dependent parameters ($\tilde{R}$ and η_∞) are available for elements $Z = 1$ through $Z = 92$ in the PENELOPE documentation[7, p. 58].

With the cross section expressed by Eq. (1.11), the macroscopic cross section for pair production at photon energy $k > 2m_ec^2$ is constructed as

$$\Sigma_{pp}(k) = \int_{\kappa^{-1}}^{1-\kappa^{-1}} \left(N_H \frac{d\sigma_{pp}(Z=1,k)}{d\epsilon} + N_C \frac{d\sigma_{pp}(Z=6,k)}{d\epsilon}\right) d\epsilon\ . \tag{1.20}$$

If $k \leq 2m_ec^2$, then Σ**pp[**k**]** returns 0 (pair production is forbidden).

1.3.2 Sampling Algorithm

The sampling procedure for pair production utilizes an algorithm detailed in PENELOPE.[7] The algorithm is invoked by the command **ppRXN[**k**]**, returning a list of the form: $\{\{-1, E_e, \theta_e, \phi_e\}, \{+1, E_p, \theta_p, \phi_p\}\}$.

The procedure first samples whether the pair production occurs in the vicinity of a hydrogen or carbon atom, by splitting the integral of Eq. (1.20) into $\Sigma_{pp} = \Sigma_H + \Sigma_C$ and choosing the target atom based on these two point probabilities. The energy of the produced electron is then sampled according to the following rules:

[4] $\tilde{R} = Rm_ec/\hbar$, for screening radius R.

(i) The parameters u_1, u_2 describing the shape of the differential cross section are calculated by

$$u_1 = \frac{2}{3}\left(\frac{1}{2} - \frac{1}{\kappa}\right)^2 \phi_1(1/2) \,, \qquad u_2 = \phi_2(1/2) \,, \tag{1.21}$$

using the same definitions as in Eq. (1.14).

(ii) A random number $r_1 \in [0,1]$ is generated, and an integer value $i = 1, 2$ is sampled according to the point probabilities

$$p_1 = \frac{u_1}{u_1 + u_2} \,, \qquad p_2 = \frac{u_2}{u_1 + u_2} \,, \tag{1.22}$$

accepting $i = 1$ if $0 < r_1 < p_1$, else $i = 2$.

(iii) A random number $\xi_1 \in [0,1]$ is generated, and the parameter ϵ is sampled using the formula

$$\epsilon = \begin{cases} \frac{1}{2} + \left(\frac{1}{2} - \frac{1}{\kappa}\right)(2\xi - 1)^{1/3}, & \text{if } i = 1. \\ \frac{1}{\kappa} + \left(\frac{1}{2} - \frac{1}{\kappa}\right)2\xi, & \text{if } i = 2. \end{cases} \tag{1.23}$$

If $i = 1$, then $\xi_1 \in [0.5, 1]$ to prevent imaginary values of ϵ arising from the cube root term.

(iv) A random number $\xi_2 \in [0,1]$ is generated, and the rejection function $U_i(\epsilon)$ is calculated from

$$U_1(\epsilon) = \frac{\phi_1(\epsilon)}{\phi_1(1/2)} \,, \qquad U_2(\epsilon) = \frac{\phi_2(\epsilon)}{\phi_2(1/2)} \,. \tag{1.24}$$

The sampled value of ϵ is accepted if $\xi_2 \leq U_i(\epsilon)$. Otherwise, return to step (ii).

This procedure samples values of ϵ with greater than 70% efficiency near the threshold $2m_e c^2$, and increases in efficiency with increasing photon energies.

The electron's kinetic energy is set by $T_e = k\,\epsilon - m_e c^2$. By conservation of energy, the positron has kinetic energy $T_p = k - T_e - 2m_e c^2$. Because the interaction involves three bodies (nucleus, electron, and positron), the outgoing polar angles relative to the direction of the incident photon are sampled independently by an inverse transform method. Generating two random numbers $\xi_\pm \in [0,1]$, the polar angles of the electron and positron are calculated by

$$\theta = \arccos \frac{2\xi_\pm - 1 + \beta_\pm}{(2\xi_\pm - 1)\beta_\pm + 1} \,, \tag{1.25}$$

where $\beta_\pm$ is the particle's velocity in units of c. The produced particles are not necessarily coplanar, so ϕ_e and ϕ_p are each randomly chosen from 0 to 2π.

1.4 Event Prediction Module

The processes described in Sections 1.1, 1.2, and 1.3 are compiled in a single module for photon simulation in **MaPLE**. The module is invoked by the command γ**predict[**k**]**, returning a list of the form $\{s, i\}$, where s is the distance traveled by the photon and $i = 1, 2, 3$ specifies the type of interaction it experiences.

The program γ**predict[**k**]** first assembles a total macroscopic cross section, $\Sigma_t = \Sigma_c + \Sigma_{pe} + \Sigma_{pp}$, using Σ**compton[**k**]**, Σ**pe[**k**]**, and Σ**pp[**k**]**. The distance s traveled by the photon is then sampled by generating a random number $\xi \in [0, 1]$ and setting

$$s = -\ln \xi / \Sigma_t \,. \tag{1.26}$$

To sample the type of interaction, a random number $r_1 \in [0, \Sigma_t]$ is generated. If $r_1 < \Sigma_c$, the photon undergoes Compton scattering, represented by the 'interaction number' $i = 1$. If $\Sigma_c < r_1 < (\Sigma_c + \Sigma_{pe})$, photoelectric absorption occurs, and $i = 2$. If $(\Sigma_c + \Sigma_{pe}) < r_1 < \Sigma_t$, pair production occurs, which is labeled by $i = 3$.

If traveling the distance s takes the photon outside of the detector volume, it is 'terminated', and the energy it carries is lost (i.e., assumed to be unabsorbed by the scintillator). Otherwise, the photon is moved forward by s, the interaction is sampled using **comptonRXN[**k**]**, **peRXN[**k**]**, or **ppRXN[**k**]**, and the particle properties are modified accordingly.

1.5 Tabulation

The macroscopic cross sections provided in `photontable.csv` cover photon energies from $k = 0.05$ MeV up to $k = 120$ MeV in increments of 0.05 MeV. If a wider range or finer partition is desired, you can generate your own table by invoking the command **intphoton[**k_i**,** $filename$**]**. The first input $k_i = \{k_1, k_2, ..., k_n\}$ is a list of photon energies at which the three macroscopic cross sections are integrated. The program takes each k_i value and constructs a table with entries of the form $\{k_i, \Sigma_c(k_i), \Sigma_{pe}(k_i), \Sigma_{pp}(k_i)\}$. The second input, $filename$, is a string that specifies how the new table should be saved. At its last step, the program automatically exports the new table to the 'Tables' folder, under the name $filename.csv$. Note that the program carries out a large number of complicated integrations and, depending on the size of k_i, may take up to several hours to complete its execution.

Chapter 2

Electron and Positron Interactions

The following definitions are used throughout this chapter:

$m_e c^2$	= electron rest mass energy
r_0	= classical electron radius
α	= fine structure constant
T	= incident electron (or positron) kinetic energy
τ	$= T/m_e c^2$ = reduced incident electron (or positron) energy
T'	= transferred kinetic energy from incident particle to target particle
Z	= atomic number of target atom
β	$= v/c$ = electron (or positron) velocity in units of c
γ	$= 1/\sqrt{1-\beta^2}$ = Lorentz factor

Electrons and positrons are simulated by **MaPLE** as undergoing four interactions: Inelastic scattering, bremsstrahlung photon emission, positron-electron annihilation, and multiple elastic scattering. Compared to photon simulation, electron and positron simulation is much more difficult, because the extremely high number of interactions suffered by charged particles traversing matter makes point-to-point simulation impractical.

The approach used in **MaPLE** is to group interactions involving *small* transfers of energy, and treat them as occurring continuously along each step. The net effects of these 'soft' collisions are expressed as energy deposited by the incident particle to the surrounding detector material. 'Hard' collisions involving *large* transfers of energy are simulated explicitly using similar methods as with photons. This 'mixed-class' approach prevents the high number of soft collisions from overwhelming the computation and results in little cost to accuracy.

The mixed-class approach is used in simulating inelastic scattering and bremsstrahlung emission. In the former, an incident electron or positron transfers some kinetic energy T' to an atomic electron, dubbed the 'secondary electron'. The emission of the secondary electron is only simulated explicitly if the energy transferred T' is greater than a specified cutoff energy T_c. Similarly,

photons produced in bremsstrahlung emission are only simulated explicitly if their energy k exceeds a specified cutoff k_c. The movement of sub-threshold[1] secondary particles is ignored, because they are assumed to be absorbed within a short distance of the interaction.

Macroscopic cross sections and other important values for electron/positron simulation are provided in the tables `bremstable.csv` and `collstable.csv`, pertaining to bremsstrahlung and collisional interactions, respectively. The tables cover incident electron/positron kinetic energies from $T = 0.01$ MeV up to $T = 200$ MeV in increments of 0.01 MeV, with cutoffs $T_c = 0.2$ MeV and $k_c = 0.01$ MeV, and are loaded into mathematica under the symbolic names **`bremstable`** and **`collstable`**. If a wider energy range, finer partitioning, or different choice of cutoffs is desired, you can generate your own tables with the programs detailed in Section 2.4. A third table, `NIST.dat`, contains values related to the passage of electrons in PVT from NIST's EStar database[1]; it is loaded into mathematica under the symbolic name **`NIST`**.

2.1 Inelastic Scattering

Møller scattering refers to e^-e^- inelastic scattering, with the target atomic electron treated as free and at rest. The incident electron, with total energy E_e, transfers some kinetic energy $T' > T_c$ to the target electron, and both are scattered to different angles. Because electrons are indistinguishable particles, the electron with higher final energy is considered to be the 'original', incident particle. This imposes a kinetic energy limit of $T = 2T_c$ on the incident electron, below which hard Møller scattering cannot occur.

Bhabha scattering refers to e^+e^- inelastic scattering, in which an incident positron with total energy E_p transfers some kinetic energy $T' > T_c$ to the target electron. The particles *are* distinguishable, so the positron can transfer almost all of its kinetic energy to the electron; the kinetic energy limit for Bhabha scattering is $T = T_c$.

2.1.1 Sub-threshold Collisional Energy Losses

Sub-threshold inelastic collisional energy losses for electrons and positrons with kinetic energy T are invoked by the commands **`eLcoll[`**T**`]`** and **`pLcoll[`**T**`]`**, respectively. These commands return a value for $L^{\pm}_{coll}$, the average energy loss per unit path length (MeV cm^{-1}) due to sub-threshold inelastic collisions for electrons or positrons.

The values of $L^{\pm}_{coll}$ come from the Berger-Seltzer formula:

$$L^{\pm}_{coll} = \frac{2\pi\, r_0^2\, m_e c^2 N_e}{\beta^2}\left[\ln\frac{2(\gamma+1)}{(I/m_e c^2)^2} + G^{\pm}(\tau,\tau_{up}) - \delta\right], \tag{2.1}$$

where $N_e = 3.33 \times 10^{23}$ cm^{-3} is the electron number density in PVT and $I = 64.7$ eV is the mean excitation potential of PVT. The $G^{\pm}$ functions reflect

[1] Secondary electrons with kinetic energy $T < T_c$, and photons with energy $k < k_c$.

the differences in scattering for positrons and electrons and are defined by:

$$G^+(\tau,\tau_{up}) = \ln(\tau\tau_{up}) - \frac{\tau_{up}^2}{\tau}\left[\tau + 2\tau_{up} - \frac{3\tau_{up}^2 y}{2} - \left(\tau_{up} - \frac{\tau_{up}^3}{3}\right)y^2 - \left(\frac{\tau_{up}^2}{2} - \tau\frac{\tau_{up}^3}{3} + \frac{\tau_{up}^4}{4}\right)y^3\right], \tag{2.2}$$

$$G^-(\tau,\tau_{up}) = -1 - \beta^2 + \ln\left((\tau-\tau_{up})\tau_{up}\right) + \frac{\tau}{\tau-\tau_{up}} + \frac{1}{\gamma^2}\left[\frac{\tau_{up}^2}{2} + (2\tau+1)\ln\left(1-\frac{\tau_{up}}{\tau}\right)\right], \tag{2.3}$$

where $y = 1/(\gamma+1)$, $\tau = T/m_e c^2$, and $\tau_{up} = \min(\tau_c, \tau_{max})$. Here, the reduced cutoff energy $\tau_c = T_c/m_e c^2$ and the reduced maximum transferred energy $\tau_{max} = \tau$ or $\tau/2$ for positrons or electrons, respectively. The δ term is an empirical correction for the density effect[2]; its value is interpolated from the table **NIST**.

2.1.2 Total Cross Sections

The macroscopic cross sections for hard Møller and Bhabha scattering, Σ_m and Σ_b, are invoked by the commands Σ**moller[**T**]** and Σ**bhabha[**T**]**, interpolating from **collstable**. Due to the cutoff, Σ**moller[**T**]** returns 0 if $T \le 2T_c$, and Σ**bhabha[**T**]** returns 0 if $T \le T_c$.

The values of Σ_m are calculated from the Møller scattering cross section, which is differential in the kinetic energy T' transferred to the target electron:

$$\frac{d\sigma_m}{dT'} = \frac{2\pi r_0^2}{\beta^2}\frac{m_e c^2}{T'^2}\left[1 + \frac{T'^2}{(T-T')^2} + \frac{\tau^2\,T'^2}{(\tau+1)^2\,T^2} - \frac{2\tau+1}{(\tau+1)^2}\frac{T'}{T-T'}\right]. \tag{2.4}$$

Due to Fermi statistics, the target electron can only receive up to half of the kinetic energy carried by the incident electron. Thus, the integration is carried out as

$$\Sigma_m(T) = N_e \int_{T_c}^{T/2} \frac{d\sigma_m}{dT'} dT' \,. \tag{2.5}$$

The values of Σ_b are calculated from the Bhabha scattering cross section, which is differential in the kinetic energy T' transferred to the target electron:

$$\frac{d\sigma_b}{dT'} = \frac{2\pi\, r_0^2\, m_e c^2}{T^2}\left[\left(\frac{1}{\epsilon^2\beta^2} - \frac{B_1}{\epsilon}\right) + B_2 + \epsilon(\epsilon B_4 - B_3)\right], \tag{2.6}$$

where $\epsilon = T'/T$ and the remaining parameters are defined as:

[2] A reduction in collisional energy losses due to polarization of the medium by the electric field of the incident particle.

$$y = (\tau+2)^{-1}\,, \qquad \beta^2 = \frac{\tau(\tau+2)}{(\tau+1)^2}\,,$$
$$B_1 = 2 - y^2\,, \qquad B_2 = (1-2y)(3+y^2)\,,$$
$$B_3 = B_4 + (1-2y)^2\,, \qquad B_4 = (1-2y)^3\,, \tag{2.7}$$

with reduced positron kinetic energy $\tau = T/m_e c^2$. This time, the integration is carried out over the full range of the positron's kinetic energy:

$$\Sigma_b(T) = N_e \int_{T_c}^{T} \frac{d\sigma_b}{dT'} dT'\,. \tag{2.8}$$

2.1.3 Sampling Algorithms

Sampling the Møller and Bhabha interactions is done by invoking the commands **mollerRXN[**E_e**,**T_c**]** and **bhabhaRXN[**E_p**,**T_c**]**, which utilize algorithms from EGSnrc.[6]

The procedure for Møller scattering is based on a change of variables to $\epsilon = T'/T$, which ranges from $\epsilon_0 = T_c/T$ to $\epsilon = 1/2$:

(i) A random number $r_1 \in [0,1]$ is generated, and ϵ is sampled by assigning

$$\epsilon = \frac{T_c}{T - (T-2T_c)r_1}\,. \tag{2.9}$$

(ii) Another random number $r_2 \in [0,1]$ is generated, and the rejection function $g(\epsilon)$ is calculated from

$$g(\epsilon) = \frac{1 + g_2\,\epsilon^2 + r(r-g_3)}{g_{max}}\,, \tag{2.10}$$

where

$$g_{max} = 1 + \frac{5}{4}g_2\,, \qquad g_2 = \frac{\tau^2}{(\tau+1)^2}\,, \qquad g_3 = \frac{2\tau+1}{(\tau+1)^2}\,, \qquad r = \frac{\epsilon}{1-\epsilon}\,, \tag{2.11}$$

with reduced kinetic energy $\tau = T/m_e c^2$.

(iii) If $r_2 \le g(\epsilon)$, we accept the value of ϵ. Otherwise, we return to step (i).

With ϵ sampled, the energy transferred to the target electron is $T' = \epsilon\,T$. In a two-body collision with particles of equal mass, the polar angular deflection of the particle with higher final energy, relative to the initial direction of the incident particle, is given by

$$\theta_{hi}(T') = \arccos\sqrt{\frac{T-T'}{T}\frac{T+2m_e c^2}{T-T'+2m_e c^2}}\,. \tag{2.12}$$

Conversely, the polar angular deflection of the particle with lower final energy is given by

$$\theta_{low}(T') = \arccos\sqrt{\frac{T'}{T}\frac{T+2m_ec^2}{T'+2m_ec^2}}\ . \tag{2.13}$$

By convention, the incident electron has higher final energy, and so is scattered by polar angle $\theta_1 = \theta_{hi}(T')$; the target electron is scattered by polar angle $\theta_2 = \theta_{low}(T')$. Due to conservation of momentum in the scattering plane, the incident and target electrons are scattered to opposite azimuthal angles; $\phi_1 \in [0,\pi]$ is chosen randomly, and $\phi_2 = \phi_1 + \pi$. The final energies of the incident and target electrons are set to $E_1 = E_e - T'$ and $E_2 = T' + m_ec^2$, respectively. Thus, the command **`mollerRXN[`**E_e, T_c**`]`** returns a list of the form: $\big\{\{-1, E_1, \theta_1, \phi_1\}, \{-1, E_2, \theta_2, \phi_2\}\big\}$, describing the outcome of the scattering event.

The sampling procedure for Bhabha scattering, using the same parameterization, is as follows:

(i) A random number $r_1 \in [0,1]$ is generated, and ϵ is sampled by assigning

$$\epsilon = \frac{T_c}{T-(T-T_c)r_1}\ . \tag{2.14}$$

(ii) Another random number $r_2 \in [0,1]$ is generated, and the rejection function $g(\epsilon)$ is calculated from

$$g(\epsilon) = 1 - \beta^2\epsilon\Big(B_1 - \epsilon\left(B_2 - \epsilon\left(B_3 - \epsilon B_4\right)\right)\Big)\ , \tag{2.15}$$

using the definitions in Eq. (2.7).

(iii) If $r_2 \leq g(\epsilon)$, we accept the value of ϵ. Otherwise, return to step (i).

The outgoing energy of the positron is set to $E_p' = T - T' + m_ec^2$ and the scattered electron energy is set to $E_e = T' + m_ec^2$. The polar angular deflections for the positron and electron, θ_p and θ_e, are calculated from Eqs. (2.12) or (2.13), depending on the relative sizes of their outgoing energies. As before, the azimuthal scattering angles are chosen randomly and opposite to each other. The command **`bhabhaRXN[`**E_p, T_c**`]`** returns a list of the form: $\big\{\{+1, E_p', \theta_p, \phi_p\}, \{-1, E_e, \theta_e, \phi_e\}\big\}$, representing the outcome of the event.

2.2 Bremsstrahlung Emission

Bremsstrahlung or 'braking radiation' refers to photon emission due to the deceleration of a charged particle as it is deflected from its path by another charged particle. Positrons and electrons experience bremsstrahlung emission through interactions with atomic nuclei and bound electrons. Bremsstrahlung is treated in a mixed-class approach, with the emitted photons modeled explicitly if their energy k exceeds the production cutoff k_c. Bremsstrahlung emission with $k < k_c$ is interpreted as a continuous process of radiative energy loss occurring along the path of the particle.

2.2.1 Sub-threshold Radiative Energy Losses

For electrons or positrons with kinetic energy T, the sub-threshold radiative energy loss is invoked by the commands **`eLrad[`**T**`]`** and **`pLrad[`**T**`]`**, respectively. These commands return a value for $L^{\pm}_{rad}$, the average energy loss per unit path length (MeV cm^{-1}) due to sub-threshold bremsstrahlung emission for electrons or positrons.

For an electron with total energy E_e incident on an atom with atomic number Z, the radiative energy loss is given by the bremsstrahlung cross section, which is differential in the photon energy k:

$$\frac{d\sigma_{brems}}{dk} = \frac{r_0^2\,\alpha\,Z\big[Z+\xi(Z)\big]}{k}\left[\left(1+\frac{(E_e-k)^2}{{E_e}^2}\right)\left(\phi_1(\delta)-\frac{4}{3}\ln(Z)-\tilde{f}_c\right) - \frac{2}{3}\frac{E_e-k}{E_e}\left(\phi_2(\delta)-\frac{4}{3}\ln(Z)-4\tilde{f}_c\right)\right], \quad (2.16)$$

using the parameterizations

$$\delta = 272\,Z^{-1/3}\Delta \qquad \text{and} \qquad \Delta = \frac{k\,m_e c^2}{2E_e(E_e-k)}\,, \quad (2.17)$$

with coulomb corrections $\tilde{f}_c$, f_c, and triplet correction ξ:

$$\tilde{f}_c = \begin{cases} f_c\,, & k \geq 50 \text{ MeV} \\ 0\,, & k < 50 \text{ MeV} \end{cases},$$

$$f_c = (\alpha Z)^2 \sum_{\nu=1}^{\infty} \frac{1}{\nu\big(\nu^2+(\alpha Z)^2\big)}\,,$$

$$\xi(Z) = \frac{L_r'}{L_r - f_c}\,, \quad (2.18)$$

where L_r and L_r' are Tsai's radiation logarithms:

$$L_r = \begin{cases} \ln(184.15\,Z^{-1/3})\,, & Z > 4 \\ 5.310\,, & Z = 1 \end{cases},$$

$$L_r' = \begin{cases} \ln(1194\,Z^{-2/3})\,, & Z > 4 \\ 6.144\,, & Z = 1 \end{cases}. \quad (2.19)$$

The functions ϕ_1 and ϕ_2 account for screening effects, approximated to a Thomas-Fermi potential by

$$\phi_1(\delta) = \begin{cases} 20.867 - 3.242\delta + 0.625\delta^2\,, & \delta \leq 1 \\ 21.12 - 4.184\ln(\delta+0.952)\,, & \delta > 1 \end{cases},$$

$$\phi_2(\delta) = \begin{cases} 20.029 - 1.93\delta - 0.086\delta^2\,, & \delta \leq 1 \\ \phi_1(\delta)\,, & \delta > 1 \end{cases}. \quad (2.20)$$

To calculate the radiative energy loss, an empirical correction term is first applied to $d\sigma_{brems}/dk$. This correction takes the form of

$$A(E_e, Z) = \frac{M_1(E_e, Z)}{M_1^{NIST}(E_e, Z)} \,, \tag{2.21}$$

where M_1 is the first moment of the bremsstrahlung cross section:

$$M_1 = \int_{k_{min}}^{k_{max}} k \frac{d\sigma_{brems}}{dk} dk \,, \tag{2.22}$$

while M_1^{NIST} is the same moment, using the radiative energy losses provided by NIST's ESTAR database.[1]

For electrons, the combined radiative energy loss due to soft bremsstrahlung production from both hydrogen and carbon atoms is constructed as

$$\begin{aligned} L_{rad}^{-} = \int_0^{k_c} \Bigg(& N_H \, k \, A(E_e, Z=1) \, \frac{d\sigma_{brems}(E_e, Z=1)}{dk} dk \\ & + N_C \, k \, A(E_e, Z=6) \frac{d\sigma_{brems}(E_e, Z=6)}{dk} dk \Bigg) \,. \end{aligned} \tag{2.23}$$

The radiative energy loss for positrons L_{rad}^{+} uses the same construction, except that the cross section $d\sigma_{brems}/dk$ is first multiplied by the scaling factor F_p:[3]

$$\begin{aligned} F_p(E_e, Z) = 1 - \exp \big[& (-1.2359 \times 10^{-1} \, t + 6.1274 \times 10^{-2} \, t^2) \\ & - (3.1516 \times 10^{-2} \, t^3) + (7.7446 \times 10^{-3} \, t^4) \\ & - (1.0595 \times 10^{-3} \, t^5) + (7.0568 \times 10^{-5} \, t^6) \\ & - (1.8080 \times 10^{-6} \, t^7) \big] \,, \end{aligned} \tag{2.24}$$

where

$$t = \ln \left(1 + \frac{10^6}{Z^2} \frac{E_e - m_e c^2}{m_e c^2} \right) . \tag{2.25}$$

2.2.2 Total Cross Sections

Macroscopic cross sections for hard bremsstrahlung emission depend on the charge of the incident particle and the type of target atom. For electrons, Σ_{eH} and Σ_{eC} represent hard bremsstrahlung emission from hydrogen and carbon atoms, respectively; for positrons, the cross sections are Σ_{pH} and Σ_{pC}. For electrons and positrons with incident kinetic energy T, the cross sections are invoked by the commands Σ**eHbrems[**T**]**, Σ**eCbrems[**T**]**, Σ**pHbrems[**T**]**, and Σ**pCbrems[**T**]**, which interpolate from **bremstable**.

[3] F_p represents the ratio of the strength of the bremsstrahlung effect for positrons and electrons, and is accurate to within 0.05% of empirically tabulated values.

The macroscopic cross sections are based on $d\sigma_{brems}/dk$ as expressed in Eq. (2.16). If $T \leq k_c$, then the cross sections are 0, and hard bremsstrahlung is forbidden. Otherwise, the cross sections are constructed as:

$$\begin{aligned}
\Sigma_{eH} &= N_H \int_{k_c}^{T} A(E_e, Z=1) \frac{d\sigma_{brems}(E_e, Z=1)}{dk} dk \ , \\
\Sigma_{eC} &= N_C \int_{k_c}^{T} A(E_e, Z=6) \frac{d\sigma_{brems}(E_e, Z=6)}{dk} dk \ , \\
\Sigma_{pH} &= N_H \int_{k_c}^{T} A(E_p, Z=1)\, F_p(E_p, Z=1) \frac{d\sigma_{brems}(E_p, Z=1)}{dk} dk \ , \\
\Sigma_{pC} &= N_C \int_{k_c}^{T} A(E_p, Z=6)\, F_p(E_p, Z=6) \frac{d\sigma_{brems}(E_p, Z=6)}{dk} dk \ .
\end{aligned} \tag{2.26}$$

2.2.3 Sampling Algorithm

For a particle with charge chg and total energy E, incident on an atom with atomic number Z, and with bremsstrahlung production cutoff k_c, bremsstrahlung events are sampled by invoking the command **`bremsRXN[`**chg, E, Z, k_c**`]`**. This program first samples the emitted photon energy k, and then its polar angular deflection θ_γ.

The sampling procedure for k is based on Eq. (2.16) and comes from EGSnrc[6]:

(i) The value of $b = \ln(T/k_c)$ is calculated, and a random number $r_1 \in [0, 1]$ is generated. The photon energy k is sampled by assigning

$$k = k_c \, e^{r_1 \, b} \ . \tag{2.27}$$

(ii) The values of R and R_{max} are calculated from

$$\begin{aligned}
R(k, Z) = &\left(1 + \frac{(E-k)^2}{E^2}\right)\left(\phi_1(\delta) - \frac{4}{3}\ln Z - 4\tilde{f}_c\right) \\
&- \frac{2}{3}\frac{E-k}{E}\left(\phi_2(\delta) - \frac{4}{3}\ln Z - 4\tilde{f}_c\right) \ , \\
R_{max}(k) = &\ 28.381 - \frac{4}{3} Z_v \ ,
\end{aligned} \tag{2.28}$$

using the same parameters as in Eq. (2.16), and where

$$Z_v = \sum_i p_i Z_i \big(Z_i + \xi(Z_i)\big)\left(\frac{1}{3}\ln Z_i + \tilde{f}_c\right) \ , \tag{2.29}$$

where p_i is the normalized fraction of atoms of type i in the material (for PVT, we just have hydrogen and carbon).

(iii) Another random number $r_2 \in [0,1]$ is generated. If $r_2 \leq R/R_{max}$, we accept the value of k. Otherwise, return to step (i).

The sampling procedure for θ_γ also comes from the EGSnrc documentation:

(i) The maximum of the function $f(y)$ is calculated, with $f(y)$ defined as

$$f(y) = \left[\frac{16y^2 r}{(y^2+1)^2} - (1+r)^2 + \left(1 + r^2 - \frac{4y^2 r}{(y^2+1)^2}\right)\ln M(y)\right], \quad (2.30)$$

with

$$M(y) = \left[\Delta^2 + \left(\frac{Z^{1/3}}{111(y^2+1)}\right)^2\right]^{-1}, \quad (2.31)$$

where $r = (E-k)/E$ and $\Delta = \frac{km_ec^2}{2E(E-k)}$. The maximum value, f_{max}, occurs when either $y^2 = 0$, $y^2 = 1$, or

$$y^2 = y^2_{max} = 2\beta(1+\beta)(E/m_ec^2)^2, \quad (2.32)$$

where β is the incident particle's velocity in units of c.

(ii) A random number $r_1 \in [0,1]$ is generated, and y^2 is sampled by assigning

$$y^2 = \frac{r_1\, y^2_{max}}{1 + y^2_{max}(1-r_1)}. \quad (2.33)$$

(iii) A second random number $r_2 \in [0,1]$ is generated. If $r_2 \leq f(y)/f_{max}$, we accept the sampled value of y^2. Otherwise, return to step (ii).

(iv) The polar angle θ_γ is calculated from y^2 using the transformation

$$\theta_\gamma = \arccos\left(1 - \frac{y^2}{2\, y^2_{max}}\right). \quad (2.34)$$

With k and θ_γ sampled, the photon azimuthal scattering angle $\phi_\gamma \in [0, 2\pi]$ is chosen randomly. The incident particle's direction of travel is unaltered, because the angular deflections are accounted for in the elastic scattering cross section. Thus, the command **`bremsRXN[`**chg, E, Z, k_c**`]`** returns a list of the form: $\big\{\{chg, E-k, 0, 0\}, \{0, k, \theta_\gamma, \phi_\gamma\}\big\}$, describing the outgoing particles.

2.3 Positron Annihilation

When a positron with kinetic energy T encounters an electron, the two may annihilate to produce two photons with a combined energy $k_1 + k_2 = T + 2m_ec^2$. Conservation of energy and momentum is used to determine the angular distribution of the photons.

Positron-electron annihilation can occur 'in flight' or 'at rest'. In flight annihilation is treated as a hard interaction using the macroscopic cross section; the kinetic energy T is carried through to the produced photons. At rest annihilation occurs when the positron's kinetic energy T falls below the simulation cutoff T_{cut}, effectively terminating the captured positron.

2.3.1 Total Cross Section

The macroscopic cross section for in-flight positron annihilation, Σ_{anni}, is invoked by the command Σ**anni[**T**]**, which interpolates from **collstable**. The values of Σ_{anni} are calculated from the annihilation cross section, which is differential in the energy k_1 of one of the produced photons:

$$\frac{d\sigma_{anni}}{dk_1} = \frac{\pi\, r_0^2}{\tau\,(\tau+2)}\Big[S_1(\kappa) + S_1(\tau+2-\kappa)\Big]\,, \tag{2.35}$$

where $\tau = T/m_e c^2$, $\kappa = k_1/m_e c^2$, and

$$S_1(x) = \frac{1}{x}\left(\tau + 2 + 2\frac{\tau+1}{\tau+2} - \frac{1}{x}\right) - 1\,. \tag{2.36}$$

The photon energy and polar emission angle are implicitly related through

$$k_i = \frac{m_e c^2}{1 - a\cos\theta_i}\,, \qquad a = \sqrt{\frac{\tau}{\tau+2}}\,, \tag{2.37}$$

which impose the minimum and maximum allowed photon energies

$$k_{min} = \frac{m_e c^2}{1+a}\,, \qquad k_{max}\frac{m_e c^2}{1-a}\,. \tag{2.38}$$

The macroscopic cross section Σ_{anni} is constructed as

$$\Sigma_{anni}(T) = N_e \int_{k_{min}}^{k_{max}} \frac{d\sigma_{anni}}{dk_1} dk_1\,, \tag{2.39}$$

where $N_e = 3.33 \times 10^{23}$ is the electron number density in PVT.

2.3.2 Sampling Algorithm In-Flight

In-flight annihilation is sampled by invoking the command **anniRXN[**E_p**]**, for positron total energy $E_p = T + m_e c^2$. The command returns a list of the form: $\big\{\{0, k_1, \theta_1, \phi_1\}, \{0, k_2, \theta_2, \phi_2\}\big\}$, describing the energies and scattering angles of the produced photons.

The sampling algorithm, which comes from the EGSnrc code[6], is based on a change of variables to $\epsilon = \kappa/(\tau+2)$, with τ and κ defined as in Eq. (2.35):

(i) The parameter ϵ_0, which is the minimum value of ϵ, is calculated as

$$\epsilon_0 = \frac{1}{(\tau+2)(1+a)} , \qquad a = \sqrt{\frac{\tau}{\tau+2}} , \tag{2.40}$$

and b is calculated as

$$b = \ln\left[\frac{1-\epsilon_0}{\epsilon_0}\right] . \tag{2.41}$$

(ii) A random number $r_1 \in [0,1]$ is generated, and a value of ϵ is sampled by assigning

$$\epsilon = \epsilon_0\, e^{(r_1\, b)} . \tag{2.42}$$

(iii) A second random number $r_2 \in [0,1]$ is generated, and the rejection function $g(\epsilon)$ is calculated for the sampled value of ϵ, using

$$g(\epsilon) = 1 - \frac{\left[\epsilon\,(\tau+2) - 1\right]^2}{\epsilon\left(\tau^2+4\tau+2\right)} . \tag{2.43}$$

If $r_2 \leq g(\epsilon)$, we accept the value of ϵ. Otherwise, we return to step (ii).

With ϵ sampled, we then have $k_1 = \epsilon\,(\tau+2)\,m_e c^2$. By conservation of energy, we have $k_2 = E_p + m_e c^2 - k_1$. The photon polar scattering angles θ_1, θ_2, relative to the direction of the incident positron, are calculated from the inverse of Eq. (2.37):

$$\theta_i = \arccos\left(\frac{1 - m_e c^2/k_i}{a}\right) . \tag{2.44}$$

The photon azimuthal scattering angles ϕ_1, ϕ_2 are produced randomly and in opposite directions, satisfying conservation of momentum ($\phi_1 = \phi_2 + \pi$).

2.3.3 Sampling Algorithm for At-Rest Annihilation

When a positron's kinetic energy T falls below the simulation cutoff T_{cut}, it is considered to be captured in the scintillator material, annihilating with an atomic electron. At-rest annihilation is sampled by invoking the command **`anniatrestRXN`**, returning a list of the form: $\big\{\{0, k_1, \theta_1, \phi_1\}, \{0, k_2, \theta_2, \phi_2\}\big\}$, which describes the emitted photons.

Because the system has negligible linear momentum, the photons are emitted with energies $k_1 = m_e c^2$ and $k_2 = m_e c^2$ in opposite directions. The photon polar scattering angles θ_1, θ_2 are sampled by generating a random number $r_1 \in [0,1]$ and assigning

$$\theta_1 = \arccos\big(1 - 2r_1\big) , \qquad \theta_2 = \pi - \theta_1 . \tag{2.45}$$

The photon azimuthal scattering angle $\phi_1 \in [0, \pi]$ is generated randomly, and $\phi_2 = \phi_1 + \pi$.

2.4 Tabulation

You can generate your own tables of bremsstrahlung and collisional cross section data using the integrator programs **intbrems[**$E_{ki}, k_c, filename$**]** and **intcolls[**$E_{ki}, T_c, filename$**]**. These programs carry out a high number of complicated integrations and may take several hours to run, depending on the size of the list E_{ki}.

The bremsstrahlung integrator **intbrems** takes as argument a list of kinetic energies E_{ki}, bremsstrahlung production cutoff energy k_c, and a string $filename$. For each kinetic energy value in E_{ki}, six values are calculated: the combined radiative energy loss due to soft bremsstrahlung production for electrons (L^-_{rad}) and for positrons (L^+_{rad}), and the four macroscopic cross sections for hard bremsstrahlung events ($\Sigma_{eH}, \Sigma_{eC}, \Sigma_{pH}, \Sigma_{pC}$). The program forms a table with entries of the form $\left\{E_{ki}, L^-_{rad}, L^+_{rad}, \Sigma_{eH}, \Sigma_{eC}, \Sigma_{pH}, \Sigma_{pC}\right\}$, and saves it in the 'Tables' folder, under the specified name $filename.csv$.

The collisional integrator **intcolls** takes as argument a list of kinetic energies E_{ki}, secondary electron production threshold T_c, and a string $filename$. For each kinetic energy value in E_{ki}, nine values are calculated: the elastic scattering macroscopic cross sections from hydrogen and carbon (Σ_H, Σ_C), first and second transport mean free paths from Section 3.3.3 ($\lambda_{\mathrm{el},1}, \lambda_{\mathrm{el},2}$), sub-threshold inelastic collisional energy losses for electrons and positrons (L^-_{coll}, L^+_{coll}), and macroscopic cross sections for Møller scattering, Bhabha scattering, and in-flight positron annihilation ($\Sigma_m, \Sigma_b, \Sigma_{anni}$). The program forms a table with entries of the form $\left\{E_{ki}, \Sigma_H, \Sigma_C, \lambda_{\mathrm{el},1}, \lambda_{\mathrm{el},2}, L^-_{coll}, L^+_{coll}, \Sigma_m, \Sigma_b, \Sigma_{anni}\right\}$, and saves it in the 'Tables' folder, under the specified name $filename.csv$.

Chapter 3

Particle Transport

Particles in **MaPLE** are each assigned a vector of the form:

$$\overrightarrow{p} = \{\overrightarrow{e}, \overrightarrow{x}\} = \big\{\{chg, E\}, \{R, Z, \Omega, \theta, \phi\}\big\} \; . \tag{3.1}$$

The first component $\overrightarrow{e}$ identifies the particle's charge chg[1] and energy E[2], while $\overrightarrow{x}$ identifies its position and direction: R, Z, and Ω give the particle position in cylindrical coordinates, while θ, ϕ describe its angular direction, as depicted in Figure 3.1.

3.1 Scattering and Transit Functions

The functions **`transit`** and **`scatter`** perform the geometric transformations related to particle movement and scattering.

`transit[`$\overrightarrow{x}, s$**`]`** moves a particle with directional vector $\overrightarrow{x}$ forward by distance s, returning the updated directional vector $\overrightarrow{x}'$. The values in $\overrightarrow{x}$ are transformed using trigonometry and the law of cosines, as follows:

$$\begin{aligned}
R \to R' &= \sqrt{R^2 + (s\sin\theta)^2 - 2\,R\,s\sin\theta\,\cos(\pi - \phi)}\;, \\
Z \to Z' &= Z + s\cos\theta\;, \\
\Omega \to \Omega' &= \begin{cases} \Omega + \psi, & \text{if } \phi < \pi \\ \Omega - \psi, & \text{if } \phi > \pi \end{cases}\;, \\
\phi \to \phi' &= \begin{cases} \phi - \psi, & \text{if } \phi < \pi \\ \phi + \psi, & \text{if } \phi > \pi \end{cases}\;,
\end{aligned} \tag{3.2}$$

where ψ is defined as

$$\psi = \arccos\left(\frac{R + s\sin\theta\cos\phi}{R'}\right) . \tag{3.3}$$

[1] $chg = 0$ for photons, -1 for electrons, and $+1$ for positrons.
[2] for electrons or positrons with kinetic energy T, $E = T + m_e c^2$ is the total energy.

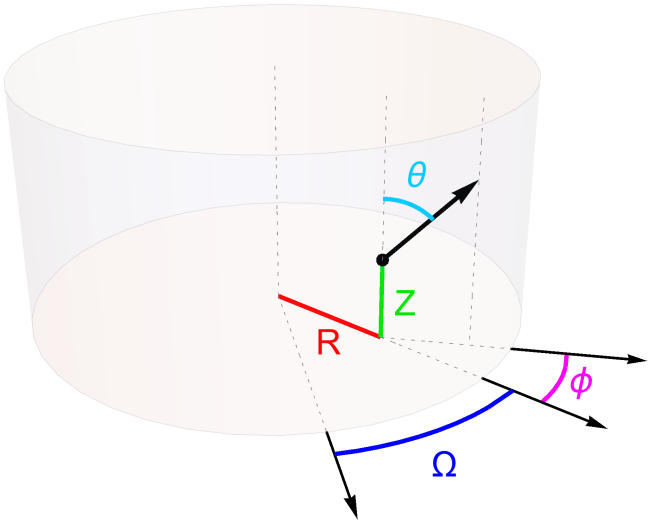

Figure 3.1: Depiction of the cylindrical coordinates used in **MaPLE**: (R, Z, Ω) specify the particle's position, while (θ, ϕ) specify its local angular direction. The cylindrical phase Ω is defined relative to an arbitrary axis.

The value of θ is unchanged by **`transit`**, because the polar angle is always defined relative to the Z-axis.

`scatter[`$\theta_i, \phi_i, \theta_{sc}, \phi_{sc}$**`]`** updates the angular direction of a particle with initial direction (θ_i, ϕ_i) that is scattered by polar angle θ_{sc} and azimuthal angle ϕ_{sc} relative to the initial direction. This is done by applying rotation matrix M to the three-dimensional cartesian vector $\big(\sin(\theta_i - \theta_{sc}),\ 0,\ \cos(\theta_i - \theta_{sc})\big)$, as depicted in Figure 3.2.

3.2 Detector Geometry and Boundary Crossing

The functions **`geotest`** and **`findexit`** are used to test if a particle remains in the detector geometry and to determine the distance to the detector boundary.

`geotest[`$R_d, H_d, \overrightarrow{x}$**`]`** returns `True` if the particle with position $\overrightarrow{x}$ is found inside the cylindrical detector with radius R_d and height H_d (cm). Otherwise, **`geotest`** returns `False`.

`findexit[`$R_d, H_d, \overrightarrow{x}, s, \epsilon$**`]`** is used to calculate the distance a particle travels before crossing the detector boundary, in cases where **`transit[`**$\overrightarrow{x}, s$**`]`** takes the particle outside of the detector. The program **`findexit`** performs an iterative bisection routine to return s', the straight-line distance to the detector boundary, with precision ϵ.

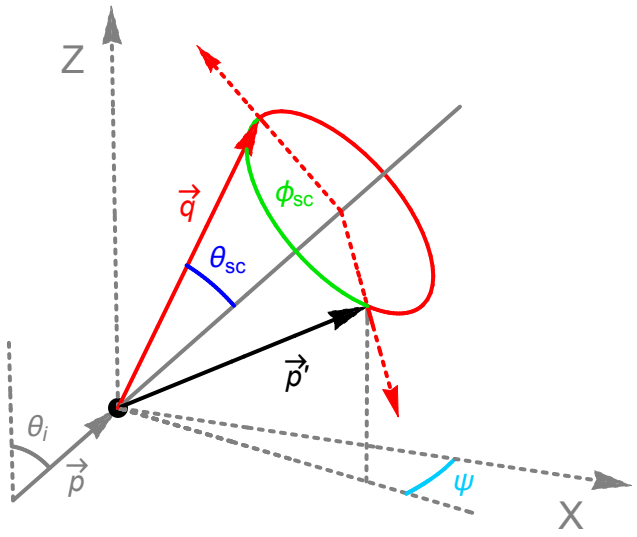

Figure 3.2: A particle $\vec{p}$ is scattered at the origin by polar and azimuthal scattering angles θ_{sc}, ϕ_{sc}. The function **scatter** performs a rotation of the vector $\vec{q} = \big(\sin(\theta_i - \theta_{sc}),\, 0,\, \cos(\theta_i - \theta_{sc})\big)$ through angle ϕ_{sc}, about the initial direction of $\vec{p}$, giving the updated particle direction $\vec{p}'$ (black arrow).

3.3 Multiple Scattering and Event Prediction Module

As a particle $\vec{p}$ travels distance s, it experiences a large number of low-angle elastic scattering events; the resulting cumulative angular deflection and lateral displacement from its initial direction of travel are expressed using a multiple scattering distribution.

The functions **eMSTEP** and **pMSTEP** combine the macroscopic cross sections from Chapter 2 with a multiple scattering algorithm in order to step electrons and positrons forward in small iterations. Both functions take as argument $\texttt{[}R_d, H_d, \vec{p}, k_c, T_c, s_{min}, T_{cut}, \epsilon\texttt{]}$[3] and return a list of the form: $\{int, \Delta E, \vec{p}'\}$, where *int* is a number codifying the type of interaction that occurs at the end of the step, ΔE is the energy deposited along the step, and $\vec{p}'$ is the state of the particle after the step.

[3]For bremsstrahlung production cutoff k_c, secondary electron production cutoff T_c, minimum step s_{min} (cm), simulation cutoff energy T_{cut}, and boundary crossing precision ϵ.

3.3.1 Step Length Selection and Energy Deposition

For a particle $\overrightarrow{p}$ with kinetic energy T, the step length s is determined by solving the equation

$$fr = \frac{\Delta E(T,s)}{T + m_e c^2} \ , \tag{3.4}$$

where $\Delta E(T,s)$ is the energy deposited along s due to sub-threshold collisional and radiative interactions (Eqs. 2.1 and 2.23). The parameter fr is the maximum fractional energy loss per step to be tolerated; if $fr = 0.05$, the particle travels a distance s over which $1/20^{\text{th}}$ of its initial energy is deposited. This prevents the energy-dependent cross sections from varying too drastically over a single step. If the value of s is less than the specified minimum step length s_{min}, s is set equal to s_{min}, which prevents excessively small step lengths at low energies.

If $L_{tot}(T)$ is the total energy loss per unit path length, then the deposited energy $\Delta E(T,s)$ is approximated over s using

$$\Delta E(T,s) = L_{tot}\left[T - L_{tot}(T)\frac{s}{2}\right]s \ . \tag{3.5}$$

The particle's final energy, on traveling s, is set to $E_f = E_i - \Delta E(T,s)$.

3.3.2 Multiple Scattering Algorithm

Multiple scattering is treated using the alternating random-hinge method developed by Bielajew[7]. The multiple scattering over s can be described exactly by the probability density $F(s;\chi)$ of the particle having a final direction in the solid angle $d\Omega$ about a direction defined by the polar angle χ:

$$F(s;\chi) = \sum_{l=0}^{\infty} \frac{2l+1}{4\pi} \exp(-s/\lambda_{\text{el},l})\, P_l(\cos\chi) \ , \tag{3.6}$$

where P_l are the Legendre polynomials and $\lambda_{\text{el},l} = (\eta\, \sigma_{\text{el},l})^{-1}$ is the l^{th} transport mean free path, with

$$\sigma_{\text{el},l} \equiv \int \big(1 - P_l(\cos\theta)\big)\frac{d\sigma_{\text{el}}}{d\Omega} d\Omega \tag{3.7}$$

for elastic scattering differential cross section $d\sigma_{\text{el}}/d\Omega$ and a density of scattering centers η.

Although Eq. (3.6) is an exact distribution, it converges too slowly for use in simulation. Instead, we sample the angular deflection from an artificial piecewise distribution, given by

$$F_a(s;\mu) = a\, U_{0,b}(\mu) + (1-a)\, U_{b,1}(\mu) \ , \tag{3.8}$$

where $U_{i,j}(\mu)$ is the normalized uniform distribution on the interval (i,j), with the polar scattering angle parameterized by $\mu = (1 - \cos\theta_{sc})/2$.

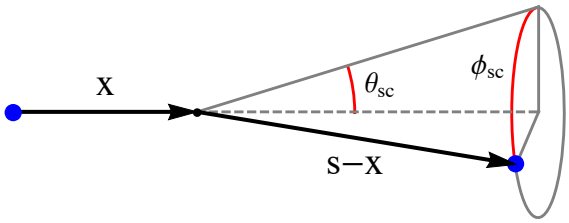

Figure 3.3: Multiple scattering step of a particle using the random hinge method. The multiple elastic scattering over s occurs at a single artificial scattering 'hinge' at random distance $x \in [0, s]$. The angle θ_{sc} is sampled at either the particle's initial or final energy. The azimuthal scattering angle ϕ_{sc} is chosen randomly from 0 to 2π, due to radial symmetry of the elastic scattering cross section.

In order to accurately represent the multiple scattering, $F_a(s;\mu)$ is constrained to reproduce the first and second moments of $F(s;\mu)$:[4]

$$\begin{aligned} \langle\mu\rangle &= \frac{1}{2}\Big(1 - \exp(-s/\lambda_{\text{el},1})\Big) \,, \\ \langle\mu^2\rangle &= \langle\mu\rangle - \frac{1}{6}\Big(1 - \exp(-s/\lambda_{\text{el},2})\Big) \,, \end{aligned} \tag{3.9}$$

this constraint sets the values of the a and b parameters to

$$a = 1 - 2\langle\mu\rangle + b \,, \qquad b = \frac{2\langle\mu\rangle - 3\langle\mu^2\rangle}{1 - 2\langle\mu\rangle} \,. \tag{3.10}$$

The use of $F_a(s;\mu)$ allows for fast sampling of the multiple scattering angular deflection with little cost to accuracy, because the details of the artificial distribution are washed out after a sufficiently large number of multiple scattering steps. The value of μ is sampled from $F_a(s;\mu)$ with a simple rejection-sampling technique, and the polar multiple scattering angle θ_{sc} is back-calculated from the parameterization of μ.

The lateral displacement of the particle is simulated by introducing an artificial 'hinge' event mid-step; the cumulative angular deflection θ_{sc} is applied at a random point along s, as depicted in Figure 3.3. To account for the energy dependence of the elastic scattering cross section, the energy loss and angular deflection over s are treated as independent processes and are simulated in random order. That is, the value of μ is sampled randomly either at the particle's initial or final energy.

3.3.3 Elastic Scattering Transport Mean Free Paths

The multiple scattering distribution $F_a(s;\mu)$ depends on the first and second transport mean free paths for elastic scattering, $\lambda_{\text{el},1}$ and $\lambda_{\text{el},2}$. The values of

[4] Based on a soft-scattering approximation to Eq. (3.6)

$\lambda_{\mathrm{el},1}$, $\lambda_{\mathrm{el},2}$ are invoked by the commands λ**1[**T**]**, λ**2[**T**]**, which interpolate from **collstable**.

As provided by the EGSnrc documentation,[6] $\lambda_{\mathrm{el},1}$ and $\lambda_{\mathrm{el},2}$ are calculated using the screened Rutherford elastic scattering cross section, which is differential in $u = \cos\theta$:

$$\frac{d\sigma_{\mathrm{el}}}{du} = \frac{2\pi\, r_0^2\, Z(Z+\xi)}{\beta^2\,\tau(\tau+2)} \frac{1}{(1-u+2\eta)^2}\ , \tag{3.11}$$

where $\tau = T/m_e c^2$ and η is the screening parameter defined by

$$\eta = \eta_0(1.13 + 3.76\,\zeta^2)\ , \qquad \eta_0 = \frac{\alpha^2 Z^{2/3}}{4\,C^2\tau(\tau+2)}\ , \qquad C = \left(\frac{9\pi^2}{128}\right)^{1/3}\ , \tag{3.12}$$

with $\zeta = (\alpha Z)/\beta$. The parameter ξ expresses the contribution to angular deflection from sub-threshold inelastic collisions:

$$\xi = 1 - \frac{1}{\bar{Z}+1}\frac{g_M(\tau,\tau_c)}{g_R(\eta)}\ , \tag{3.13}$$

where $\bar{Z}$ is the average atomic number of PVT, $\tau_c = T_c/m_e c^2$, and

$$\begin{aligned} g_M(\tau,\tau_c) = {} & \ln\frac{\tau}{2\tau_c} + \left[1 + \frac{(\tau+2)^2}{(\tau+1)^2}\right]\ln\left[\frac{2(\tau-\tau_c+2)}{\tau+4}\right] \\ & - \left[\frac{(\tau+2)^2}{4} + \frac{(\tau+2)(\tau+1/2)}{(\tau+1)^2}\right]\ln\left[\frac{(\tau+4)(\tau-\tau_c)}{\tau(\tau-\tau_c+2)}\right] \\ & + \frac{(\tau-2\tau_c)(\tau+2)}{2}\left[\frac{1}{\tau-\tau_c} - \frac{1}{(\tau+1)^2}\right]\ , \end{aligned} \tag{3.14}$$

$$g_R(\eta) = (1+2\eta)\Big[\ln\big(1+1/\eta\big) - 2\Big]\ . \tag{3.15}$$

As before, the l^{th} transport mean free path in PVT is constructed from Eq. (3.7) using the hydrogen and carbon atomic number densities N_H and N_C:

$$\lambda_{\mathrm{el},l} = \left[\int \big(1 - P_l(\cos\theta)\big) \times \left(N_H \frac{d\sigma_{\mathrm{el}}(Z=1)}{du} + N_C \frac{d\sigma_{\mathrm{el}}(Z=6)}{du}\right) du\right]^{-1}\ . \tag{3.16}$$

3.3.4 Event Prediction

At the end of each step, an event prediction routine determines whether an interaction (other than elastic scattering) takes place. The total macroscopic cross section Σ_{int} is invoked by the command **e**Σ**tot[**T**]** for electrons and **p**Σ**tot[**T**]** for positrons. The value of Σ_{int} is calculated at the average kinetic energy of the particle over s,

$$T_{avg} = \frac{E_i + E_f}{2} - m_e c^2\ . \tag{3.17}$$

The probability of an interaction occurring over s is then given by

$$P_{int} = 1 - \exp(-s\,\Sigma_{int}) \; . \tag{3.18}$$

A random number $r_1 \in [0,1]$ is generated. If $r_1 < P_{int}$, an interaction occurs, and the type of interaction is sampled based on the point probabilities

$$P_i = \frac{\Sigma_i}{\Sigma_{int}} \; , \qquad \sum_{i=1}^{n} P_i = 1 \; , \tag{3.19}$$

for the n different interactions 'in play'.

3.3.5 Particle Stepping Routine

The full stepping procedure of **eMSTEP** and **pMSTEP**, combining multiple scattering and event prediction, is carried out as follows:

(i) The step length s and energy deposition ΔE are calculated as in Section 3.3.1. The distance to the hinge point is determined by generating a random number $r \in [0,1]$ and setting $x = rs$.

(ii) The particle $\overrightarrow{p}$ is moved forward by distance x using **transit**, and its position inside or outside the detector is tested with **geotest**.

(iii) If the particle escapes the detector, the distance to the boundary s' is calculated using **findexit**, and the energy deposition over s' is calculated using Eq. (3.5). If the energy loss over s' causes E_f to fall below the simulation cutoff ($E_f < m_e c^2 + T_{cut}$), then the particle is absorbed over s', and the interaction number int is set to 1. Otherwise, the particle escapes the detector with remaining energy E_f, and int is set to 2.

If the particle remains in the detector, and if $E_f \geq m_e c^2 + T_{cut}$ (i.e. the particle is not absorbed in x), then the multiple scattering angle is sampled from Eq. (3.8), and the particle's angular direction is updated using **scatter**.

(iv) The particle is moved forward the remaining distance $s - x$ using **transit**, and its position is again checked with **geotest**. If the particle does not escape the detector, and if its final energy E_f is above the simulation cutoff, then the event prediction routine determines whether an interaction occurs.

The programs **eMSTEP** and **pMSTEP** return a list of the form $\{int, \Delta E, \overrightarrow{p}'\}$, with the values of int assigned as follows:

int	Interaction type
0	No interaction
1	Electron/positron absorption due to simulation cutoff T_{cut}
2	Electron/positron escape through detector boundary
3	Hard Møller scattering
4	Electron-Hydrogen bremsstrahlung
5	Electron-Carbon bremsstrahlung
6	Hard Bhabha scattering
7	Positron-Hydrogen bremsstrahlung
8	Positron-Carbon bremsstrahlung
9	In-flight positron annihilation

Table 3.1: Values of *int* and the associated interaction type, as returned by **eMSTEP** and **pMSTEP**.

3.4 Interpolation

To cut down on simulation time, various parameters related to particle stepping are pre-calculated at the onset of a simulation. Specifically, the step length s, energy deposition $\Delta E(T, s)$, and total interaction macroscopic cross section Σ_{int} are pre-calculated for a range of energies. For each subsequent particle step, an interpolation function is used to 'look-up' the correct value rather than carrying out the explicit calculation.

The command **setprefunctions[**E_{ki}, k_c, T_c, fr**]** returns the interpolation functions, covering a range of E_{ki} kinetic energies, with production cutoffs k_c, T_c, and fractional step parameter fr. The function returns a list of interpolation functions of the form $\{$**eStepFunc, pStepFunc, eΔEFunc, pΔEFunc, eΣtot, pΣtot**$\}$, with each function taking as argument the particle's kinetic energy E_{ki}. The functions **eStepFunc** and **pStepFunc** return the correct electron or positron step length s, **eΔEFunc** and **pΔEFunc** give the energy deposition ΔE over s due to sub-threshold radiative and collisional interactions, and **eΣtot** and **pΣtot** give the total interaction macroscopic cross section Σ_{int} for electrons and positrons, respectively.

Chapter 4

Monte Carlo Simulation

The Monte Carlo program simulates N separate muon decay events, in each case recording the total deposited energy E_{dep} from the primary particle and all produced secondary particles. Thus, a distribution of N different E_{dep} values is formed for comparison with observed distributions.

4.1 Particle Evolution

Particle 'evolution' refers to the repeated stepping and tracking of an initial particle $\overrightarrow{p}$ and all produced secondary particles, until every particle has either escaped or been absorbed in the detector. The total deposited energy E_{dep} is analogous to the pulse strength observed at the photomultiplier tube in real muon decay events.

The program **FastEvolve[**$R_d, H_d, \overrightarrow{p}, k_c, T_c, s_{min}, T_{cut}, \epsilon$**]** is used to evolve an initial particle $\overrightarrow{p}$ in a cylindrical detector of radius R_d and height H_d (both in cm), using bremsstrahlung photon and secondary electron production cutoffs k_c and T_c (both in MeV), minimum step length s_{min} (cm), kinetic energy simulation cutoff T_{cut}, and boundary crossing parameter ϵ. Because **FastEvolve** calls on interpolation functions established by **setprefunctions** in Section 3.4, the values of k_c and T_c *must* agree between the programs, otherwise forbidden interactions may be introduced.

FastEvolve repeatedly applies **eMSTEP** or **pMSTEP**, tallying the deposited energy from each multiple scattering step and tracking the particle's position in the detector. Whenever a hard interaction occurs, the associated sampling algorithm is evaluated, and the produced particle is appended to a 'stack' of secondary particles. The parameters of the primary particle are modified accordingly, and stepping is resumed until the primary either escapes or is absorbed in the detector. The same procedure is then applied to each secondary particle in the stack, until no more particles remain in the stack (the procedures of Section 1.4, along with **transit**, **scatter**, and **geotest** are used if the secondary particle is a photon). **FastEvolve** is so-named because it returns

only the total deposited energy E_{dep}; no other information is saved in the course of particle evolution, reducing simulation time.

4.1.1 Tracking Evolver

Although **`FastEvolve`** carries out particle evolution for the Monte Carlo simulation, an additional evolution program is provided for event visualization and further exploration.

`TrackingEvolve[`$R_d, H_d, \overrightarrow{p}, k_c, T_c, s_{min}, T_{cut}, \epsilon$**`]`** evolves the primary particle $\overrightarrow{p}$, recording all particle information. **`TrackingEvolve`** returns a list of the form $\{E_{dep}, esccount, evcount, tree\}$, where E_{dep} is the total deposited energy, *esccount* is a record of escaped particles, *evcount* is a record of simulated events, and *tree* is the record of all the simulated particle positions.

esccount is a list of the form $\{\{n_\gamma, E_\gamma\},\{n_p, E_p\}\}$, where n_γ is the total number of photons that escaped the detector, E_γ is the total energy carried by the escaping photons, n_p is the total number of electrons and positrons that escaped the detector, and E_p is the total energy carried by the escaping electrons and positrons. By conservation of energy, we always satisfy $E_{dep} + E_\gamma + E_p + m_e c^2 = E_i$ for a particle with initial total energy E_i.

evcount is a fifteen-element list, where the i^{th} element is the number of times that the corresponding interaction occurred. The interactions tallied in *evcount* correspond to the following indices:

i	Interaction
1	Photon evaluation
2	Electron evaluation
3	Positron evaluation
4	Compton scattering
5	Photoelectric absorption
6	Positron-electron pair production
7	Electron/positron step with no hard interaction
8	Electron/positron absorption due to simulation cutoff T_{cut}
9	Hard Møller scattering
10	Electron-Hydrogen bremsstrahlung
11	Electron-Carbon bremsstrahlung
12	Hard Bhabha scattering
13	Positron-Hydrogen bremsstrahlung
14	Positron-Carbon bremsstrahlung
15	In-flight positron annihilation

Table 4.1: Indices i of the list *evcount* and the corresponding tallied interactions.

tree is a list of n particle trajectories or *branches*, taking the form

$$tree = \{b_1, b_2, ..., b_n\} , \tag{4.1}$$

where each branch b_i is itself a list of m flattened particle vectors:

$$b_i = \{p_1, p_2, ..., p_m\}\ , \tag{4.2}$$

where $p_j = \{chg, E, R, Z, \Omega, \theta, \phi\}$ are the parameters of a given particle. Each branch represents the entire history of a given particle, from creation to absorption or escape. The first branch in $tree$, b_1, represents the trajectory of the primary electron or positron; each subsequent branch represents the trajectory of the secondary particles. When any given particle is stepped, its properties are updated, and the new parameters p_j are appended to the current branch. When a particle escapes or is absorbed, a new branch is started corresponding to the next secondary particle at the top of the stack.

4.1.2 Event Visualization

The program **`VisualizeEvent[`**$R_d, H_d, tree$**`]`** plots a 3D visualization of a given particle evolution $tree$ produced by **`TrackingEvolve`** in a cylindrical detector of radius R_d, height H_d (both in cm). One such visualization is shown in Figure 4.1 with $R_d = 10$ cm and $H_d = 40$ cm. The primary particle started as a 50 MeV electron, located at $Z = 35$ cm and directed down along the detector's axis. By default, electron branches are blue, positron branches are purple, and photon branches are red.

From Figure 4.1, it is clear that photons behave erratically, often carrying energy away from the primary particle track. This energy is sometimes redeposited to the detector via Compton scattering, while otherwise escaping the detector. The total deposited energy was $E_{dep} = 37.88$ MeV; as such, this event would appear as a lower energy than the 'true' initial value of $E_i = 50$ MeV.

4.2 Prerequisites

4.2.1 Spawning Primary Particles

The full Monte Carlo simulation produces a distribution of E_{dep} values by separately evolving N different primary particles. The initial population of primary particles is generated with the program **`spawn[`**R_d, H_d, N, m_μ**`]`**, which returns a list of N primary particles of the form $\{\overrightarrow{p_1}, \overrightarrow{p_2}, ..., \overrightarrow{p_N}\}$, for a detector of radius R_d cm, height H_d cm, and assuming muon rest mass m_μ MeV.

`spawn` assigns each particle an initial position (R_i, Z_i, Ω_i) generated randomly and isotropically throughout the detector volume. The initial angular direction (θ_i, ϕ_i) is also generated randomly and isotropically for each particle. The energy E_i of each particle is chosen randomly and uniformly from $E_{min} = m_e c^2$ to $E_{max} = (m_\mu^2 + m_e^2)c^4/2m_\mu c^2$. The charge of each particle is assigned randomly in proportion to $R_{+/-} = 1.08$, the estimated muon charge ratio (μ_+/μ_-) at sea level and at 32.5° latitude.[4] As such, electrons are produced slightly less often than positrons, a result of the fact that negative muons

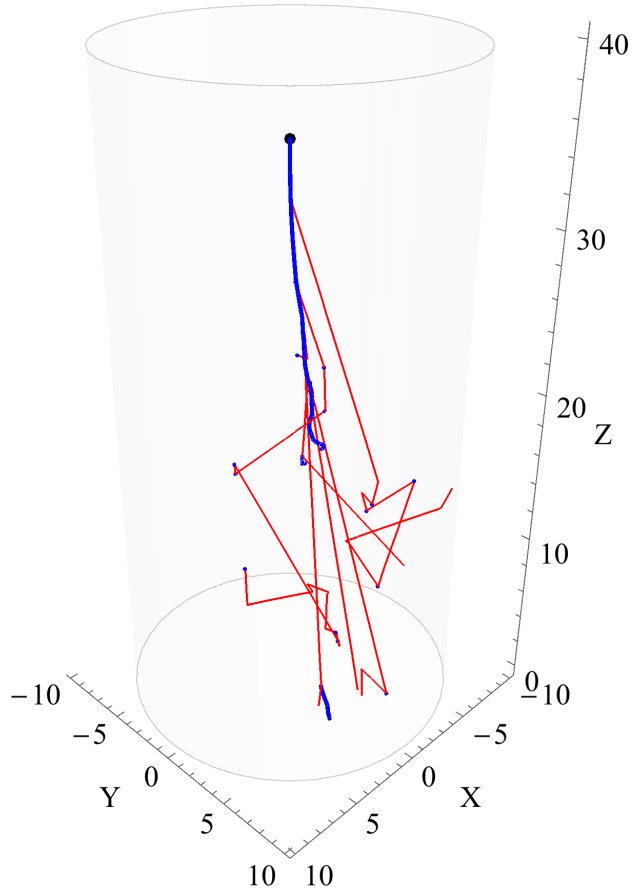

Figure 4.1: 3D Visualization of particle tracks from the evolution of a 50 MeV electron located at $Z = 35$ cm, directed down along the detector's axis, with $R_d = 10$ cm and $H_d = 40$ cm. Electron tracks are in blue, and photon tracks are in red. In this event, five photons escaped carrying a total of 7.77 MeV outside the detector, and one electron escaped carrying 3.84 MeV outside the detector. 38 photon evaluations and 167 electron evaluations were carried out in total; 118 electron steps resulted in no hard interactions. 31 instances of Compton scattering and 2 instances of photoelectric absorption occurred. 20 instances of electron absorption, 4 instances of hard Møller scattering, 1 instance of electron-Hydrogen bremsstrahlung, and 6 instances of electron-Carbon bremsstrahlung occurred. The total deposited energy was $E_{dep} = 37.88$ MeV.

experience the small but additional interaction of nuclear capture by atomic protons.[1]

4.2.2 Energy Weighting

Because **spawn** assigns energies uniformly over the interval (E_{min}, E_{max}), it does not reproduce the underlying physics of muon decay. In laboratory muon decay events, the energy of the produced electron or positron is governed by the probability distribution depicted in Figure 4.2, with higher energies being more probable than lower energies. The shape of the distribution is a result of the fact that muon decay is a three-body event.

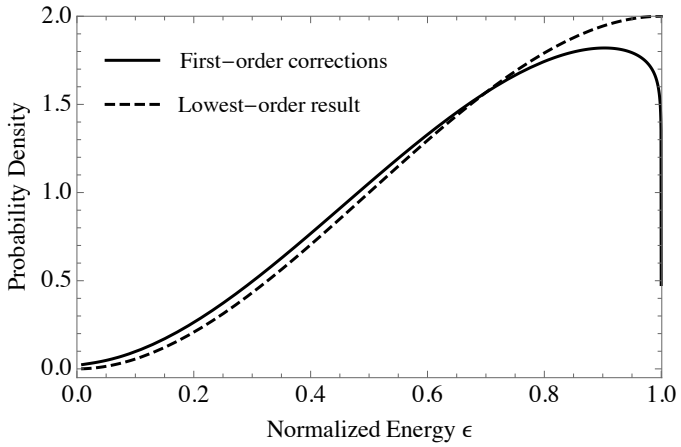

Figure 4.2: Fermi theory prediction for energy spectrum of particles produced in muon decay, in lowest-order (dotted) and with first-order radiative effects (solid) over normalized energy $\epsilon = E_i/E_{max}$.

To recover the physics of muon decay, each event with energy E_i is weighted according to the probability distribution depicted in Figure 4.2. To save time, this is done with an interpolation function, defined at the start of the Monte Carlo simulation.

The energy-weighting interpolation function is defined using the function **setEweighting[**$m_\mu c^2, c1$**]**. This function takes as argument a muon rest mass $m_\mu c^2$ MeV and partition number $c1$, and creates an evenly partitioned list of $c1$ different energies over the interval (E_{min}, E_{max}). At each energy in this list, the probability density is calculated from the analytic form of the Fermi distribution in Figure 4.2. **setEweighting** then returns an interpolation function of these values, which is much faster than using the full analytic form of the distribution. The parameter $c1$ can be set to any value; a value of two or three hundred will ensure accurate interpolation over the range of energies.

[1] Muon capture produces a neutron and a neutrino, and sometimes a radiative photon.

4.3 Monte Carlo Simulation

The command **MaPLE**$[R_d, H_d, N, m_\mu c^2, k_c, T_c, fr, s_{min}, T_{cut}, \epsilon, c1, E_{ki}, t_{cons}]$ carries out a Monte Carlo simulation of N muon decay events in a cylindrical detector of radius R_d cm and height H_d cm, assuming muon rest mass $m_\mu c^2$ MeV. The remaining simulation parameters are defined as follows:

k_c	Bremsstrahlung photon production threshold, MeV (Section 2.2)
T_c	Secondary electron production threshold, MeV (Section 2.1)
fr	Fractional energy loss parameter (Section 3.3.1)
s_{min}	Minimum electron/positron step length, cm
T_{cut}	Kinetic energy cutoff for simulation, MeV (Section 3.3.5)
ϵ	Boundary crossing precision (Section 3.2)
$c1$	Energy weighting resolution number (Section 4.2.2)
E_{ki}	Kinetic energy range of simulation (Section 3.4)
t_{cons}	Particle evolution time constraint,[2] s

MaPLE returns a list of N elements of the form $\{E_{dep}, W\}$. Each element represents an individual muon decay event, with deposited energy E_{dep} and energy weighting factor W calculated as in Section 4.2.2. The $\{E_{dep}, W\}$ values are used to form a weighted histogram of deposited energies, for comparison with the observed distribution.

MaPLE interpolates values from the tables **bremstable** and **collstable**, which are themselves calculated assuming values for k_c and T_c. The values for k_c and T_c fed to **MaPLE** *must* be the same as those assumed values; by default, the provided tables use $k_c = 0.01$ MeV and $T_c = 0.2$ MeV. Custom tables may be generated at different k_c and T_c values, as in Section 2.4.

The full procedure of **MaPLE** is carried out as follows:

(i) **setprefunctions**$[E_{ki}, k_c, T_c, fr]$ is used to calculate the particle stepping interpolation functions, as in Section 3.4.

(ii) **setEweighting**$[m_\mu c^2, c1]$ is used to calculate the energy weighting function, assigned the symbolic name **Eweighting**, as in Section 4.2.2.

(iii) A list of N primary particles is generated using **spawn**$[R_d, H_d, N, m_\mu c^2]$, as in Section 4.2.1.

(iv) Each primary particle is evolved using **FastEvolve**, as in Section 4.1. The deposited energy E_{dep} and energy weighting W are recorded at the end of each particle evolution.

[2] t_{cons} is the maximum allowed time for the evolution of a given particle. If a particle evolution takes longer than t_{cons} seconds to complete, the calculation is abandoned. This is to prevent runaway calculations or unseen errors.

Bibliography

[1] Estar: Stopping powers and ranges for electrons. http://physics.nist.gov/PhysRefData/Star/Text/method.html.

[2] B. Brau, C. May, R. Ormond, and J. Essick. Determining the muon mass in an instructional laboratory. *American Journal of Physics*, 78(1):64–70, 2010.

[3] CERN. *Physics Reference Manual*, geant4 10.1 edition, 2014.

[4] T. Coan, T. Liu, and J. Ye. A compact apparatus for muon lifetime measurement and time dilation demonstration in the undergraduate laboratory. *American Journal of Physics*, 74(2):161–164, 2006.

[5] J.H. Hubbell, H.A. Gimm, and I.Øverbø. Pair, triplet, and total atomic cross sections (and mass attenuation coefficients) for 1 mev-100 gev photons in elements z=1 to 100. *Journal of Physical and Chemical Reference Data*, 9(4), 1980.

[6] I. Kawrakow, E. Mainegra-Hing, D.W.O. Rogers, F. Tessier, and B.R.B. Walters. *The EGSnrc Code System: Monte Carlo Simulation of Electron and Photon Transport*. NRCC, 2013.

[7] OECD Nuclear Energy Agency. *PENELOPE: A Code System for Monte Carlo Simulation of Electron and Photon Transport*, 2001.